PROCEEDINGS OF SCIENCE

# Constraining Sea Quark Distributions Through $W^{\pm}$ Cross Section Ratios Measured at STAR

**M. Posik*** **(for the STAR Collaboration)**
*Temple University, Philadelphia, PA, USA*
*E-mail:* posik@temple.edu

Over the past several years the STAR experiment at RHIC has been contributing to our understanding of the proton structure. Through its instrumentation, STAR is well equipped to measure $W \rightarrow \nu + e$ in $\sqrt{s}$ = 500/510 GeV proton-proton collisions at mid-rapidity (-1.1 $\leq \eta \leq$ 1.1) . The $W$ cross section ratio ($W^+/W^-$) is sensitive to unpolarized $u$, $d$, $\bar{u}$, and $\bar{d}$ quark distributions. At these kinematics, STAR is able to measure the quark distributions near Bjorken-$x$ values of 0.1. The RHIC runs in 2011, 2012 and 2013 at $\sqrt{s}$ = 500/510 GeV saw a significant increase in delivered luminosity from previous years. This resulted in a total data sample being collected of about 352 pb$^{-1}$ of integrated luminosity. The increased statistics will lead to a higher precision measurement of the $W^+/W^-$ cross section ratio than was previously measured by STAR's 2009 run, as well as allow for a measurement of its $\eta$ dependence at mid-rapidity. Presented here is an update of the $W$ cross section ratio analysis from the STAR 2011, 2012 and 2013 runs.

*The XXIII International Workshop on Deep Inelastic Scattering and Related Subjects*
*April 27 - May 1, 2015*
*Southern Methodist University*
*Dallas, Texas 75275*

*Speaker.

© Copyright owned by the author(s) under the terms of the Creative Commons Attribution-NonCommercial-NoDerivatives 4.0 International License (CC BY-NC-ND 4.0).

http://pos.sissa.it/

PoS(DIS2015)051

## 1. Motivation

Over the past several years parton distribution functions (PDFs) have been becoming more and more precise [1, 2, 3]. However, there are still regions in which more precision data is needed which can be used to help constrain the PDFs. For example the sea quark distributions near the valence region, $x \sim$ 0.1-0.3, still have sizable uncertainties [4].

One of the data sets used to determine the anti-quark PDFs is the $\bar{d}/\bar{u}$ measurement from E866 [5], which measured $\bar{d}/\bar{u}$ to good precision at lower $x$ ($x < 0.15$). However, their precision quickly deteriorates as they approach higher $x$ ($x > 0.2$). These data suggest an interesting behavior, as $x$ increases there seems to be a transition from being $\bar{d}$ dominated to $\bar{u}$ dominated around $x \sim 0.25$. Many models are able to describe the general $\bar{d} > \bar{u}$ behavior seen at low $x$, but fail to predict the suggested $\bar{u} > \bar{d}$ transition [6]. To better determine the behavior of $\bar{d}/\bar{u}$ the experiment SeaQuest (E-906) [7] has been designed and is currently running. Through Drell-Yan scattering, SeaQuest will probe the sea quark distribution at lower $Q^2$ than E866, but increase the precision and $x$ reach of the $\bar{d}/\bar{u}$ measurement. Although this will help constrain the PDF fits, ideally one would like more data to fit from different scattering processes and $Q^2$ scales. This will help to add more independent data to global fits, and serve as a cross check of our understanding of the QCD sea.

The $W$ boson production in proton-proton collisions is also sensitive to the sea quarks. The $W^+$ boson is sensitive to the $\bar{d}$ quark, while the $W^-$ boson is sensitive to the $\bar{u}$ quarks which can be seen in equation 1.1, and probes the distribution at $Q^2 \sim M_W^2$. The leptonic decay from $W$ bosons can be detected by looking for leptons with a high transverse momentum, $p_T$, near $M_W/2$. Then a charge separation of the leptons can be used to determine which charged $W$ boson they decayed from.

$$u + \bar{d} \rightarrow W^+ \rightarrow e^+ + \nu, \;\; d + \bar{u} \rightarrow W^- \rightarrow e^- + \bar{\nu}. \tag{1.1}$$

By considering the leading order expression for the charged $W$ cross section ratio [8], $\frac{\sigma_{W^+}}{\sigma_{W^-}}$ ($R_W$), the direct relationship to the sea quarks can be seen

$$R_W \equiv \frac{\sigma_{W^+}}{\sigma_{W^-}} \sim \frac{u(x_1)\,\bar{d}(x_2) + \bar{d}(x_1)\,u(x_2)}{\bar{u}(x_1)\,d(x_2) + d(x_1)\,\bar{u}(x_2)}. \tag{1.2}$$

It should be noted that although $R_W$ can be measured at the LHC, the region of $x$ that would be probed is below the valence region near $x \sim 0.08$ (assuming a $\sqrt{s}$ = 1 TeV and $\eta$ = 0).

## 2. Experiment

The STAR experiment at RHIC [9] serves as an excellent place to measure the charged $W$ cross section ratio, which was first measured in the STAR 2009 run [10]. The STAR experiment measured $R_W$ using proton-proton collisions at center of mass energies of $\sqrt{s} = 500/510$ GeV in the mid-rapidity region ($-1.1 \leq \eta \leq 1.1$). Several sub-detectors were used to select the $W$ events and separate their charge: the time projection chamber (TPC) [11], used for particle tracking, and the barrel electromagnetic calorimeter (BEMC) [12], used to measure particle energy. A third



PoS(DIS2015)051

sub-detector, the endcap electromagnetic calorimeter (EEMC) [13], was used to estimate the background contributions. The mid-rapidity region of STAR corresponds to about $0.1 \leq x \leq 0.3$ and $Q^2 \sim M_W^2$, which could have an impact on constraining PDFs as this is the $x$ region where E866's precision starts to drop off and is the region where the data suggests that the $\bar{u}$ quark density is greater than the $\bar{d}$ quark density. STAR has taken advantage of the yearly increase in luminosity that RHIC has provided. This luminosity increase has led to roughly 352 pb$^{-1}$ of integrated luminosity being collected during the 2011-2013 runs. With the 2013 data set still under analysis, a preliminary $R_W$ result is presented using only a fraction (102 pb$^{-1}$) of the collected 2011-2013 data.

## 3. Results

The leptons from $W$ decay are selected by following the methodology previously established by STAR [10]. Several cuts which include matching high $p_T$ tracks to BEMC clusters, a series of isolation cuts used to isolate the leptons, a $p_T$-balance cut which looks for the large missing neutrino momentum, and a charge separation cut are applied to select leptons that are likely produced from $W$ decay. Figure 1 shows the application of several isolation cuts and charge separation cuts to the data. In panel a), one can see that as more isolation cuts are applied there is a decrease in background events, which populate the kinematic region $E_T < 25$ GeV, and an enhancement of the lepton signal near $E_T \sim M_W/2$. Panels b) and c) show cuts applied to the data in order to select events which have likely originated from $W^+$ or $W^-$ decays. Panel b) shows the charge separation as a function of $E_T$, while panel c) projects the charge separation as a function of $E_T$ on to the charge separation axis. The charge separation cuts are indicated by the red lines and were chosen to avoid contamination from the opposite charge.

The charged $W$ cross section ratio can be measured experimentally as

$$\frac{\sigma_{W^+}}{\sigma_{W^-}} = \frac{\left(N_O^+ - N_B^+\right)}{\left(N_O^- - N_B^-\right)} \frac{\varepsilon^-}{\varepsilon+}, \tag{3.1}$$

where $\pm$ corresponds to positively or negatively charged lepton, $N_O$ are the number of events that pass the lepton selection cuts, $N_B$ are the number of background events estimated to be contaminating the data set, and $\varepsilon$ is the efficiency at which $W$ events are detected.

Figure 2 shows the various background contributions, Monte Carlo simulation of the $W$ decay (based on Pythia 6.4.22 [14] and GEANT [15]), and a comparison of the data to Monte Carlo $W$ signal with background contributions included for the 2011 and 2012 data sets. The background contribution labeled *Second End Cap* is an estimate of the background caused by an escaping jet's $p_T$ being misidentified as the neutrino's missing $p_T$. This is predominately a QCD like background. When the final cut of $E_T > 25$ GeV is applied, there is very little background contributions from $W \to \tau + \nu$ and $Z \to ee$ decays. The background was found to be dominated by QCD background.

A Monte Carlo based on Pythia 6.4.22 [14] and GEANT [15] is used to determine the $W^{\pm}$ detection efficiencies, shown in Fig. 3. These efficiencies account for all cut and detector efficiencies. The 2011 data was found to have a higher efficiency than the 2012 data due to running at a higher luminosity rate in 2012. Running at a higher instantaneous luminosity lead to more pile-up in the TPC, which resulted in less efficient track reconstruction and hence less efficient $W$ detection.



PoS(DIS2015)051

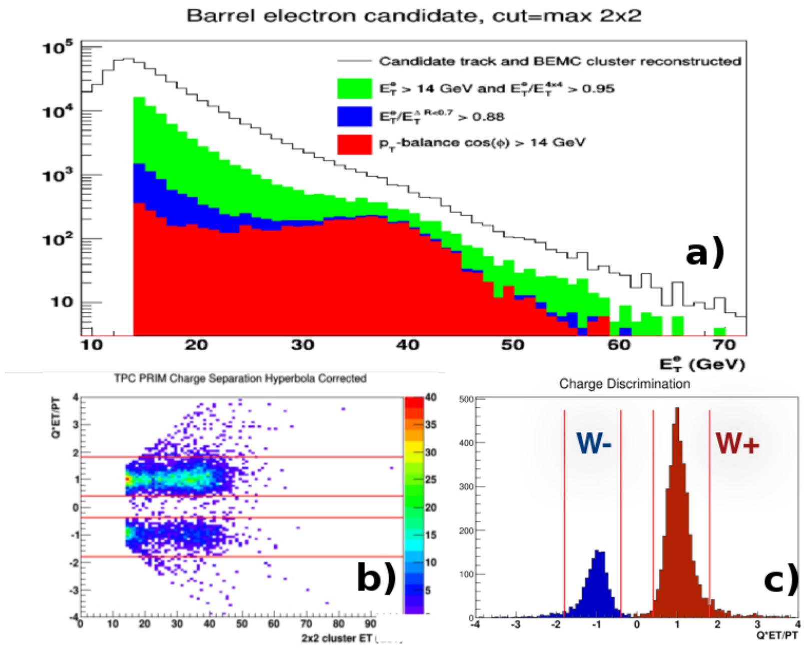


**Figure 1:** Some cuts applied to data used to select leptons which likely originated from $W$ decay. a) Application of several isolation cuts including a minimum $E_T$ cut, electron energy ratio cuts, and a signed $p_T$ cut. b) Charge separation cut vs. $E_T$. c) Projection of the charge separation vs. $E_T$ projected onto the charge separation axis.

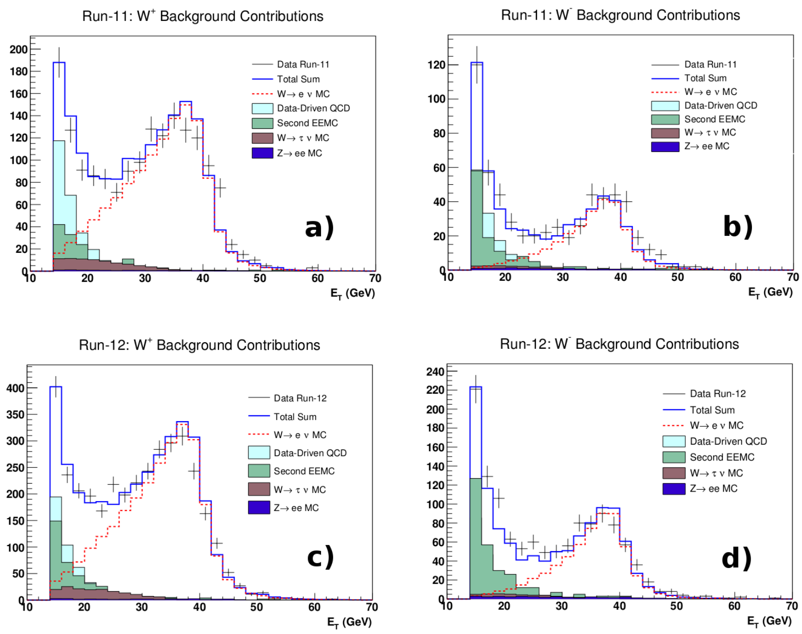


**Figure 2:** Background and Monte Carlo contributions compared to data. a) Run-11 $W^+$, b) Run-11 $W^-$, c) Run-12 $W^+$, and d) Run-12 $W^-$.

PoS(DIS2015)051

However in both data sets there was only a small ($\sim$ 1-2%) charge dependence measured between the $W^+$ and $W^-$ efficiencies, which means the $\frac{\varepsilon^-}{\varepsilon^+}$ factor will have a negligible contribution to the charged $W$ cross section ratio.

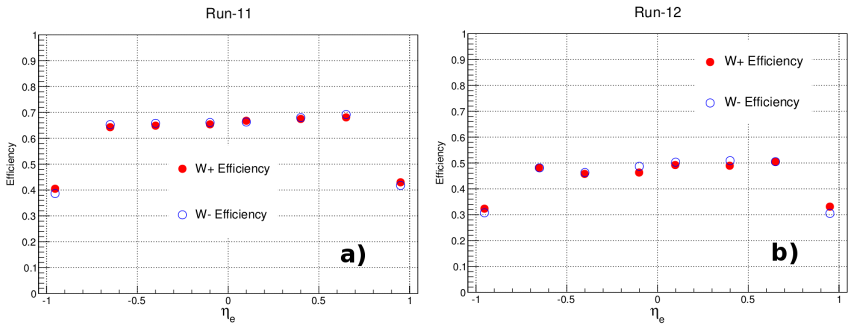


**Figure 3:** $W^+$ and $W^-$ efficiencies as a function of electron pseudo-rapidity for a) Run-11 and b) Run-12.

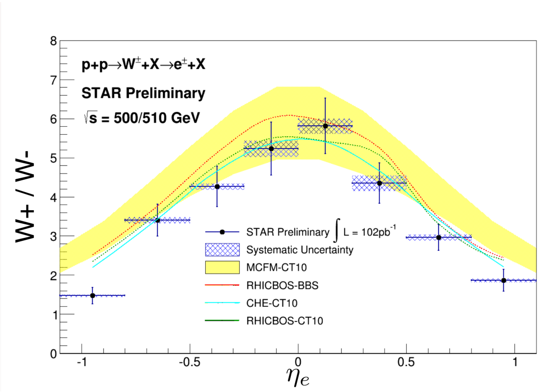


**Figure 4:** $W^+/W^-$ cross section ratio as a function of electron pseudo-rapidity.

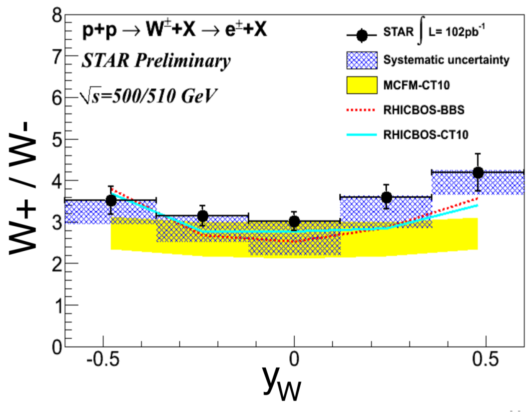


**Figure 5:** $W^+/W^-$ cross section ratio as a function of the $W$ boson rapidity.

Figure 4(5) shows the charged $W$ cross section ratio for the combined 2011 and 2012 runs, computed using equation 3.1, as a function of the electron pseudo-rapidity, $\eta_e$ ($W$ boson rapidity,

PoS(DIS2015)051

$y_W$). More information on how the $W$ boson kinematics were reconstructed can be found in [16, 17]. The error bar on the data points represents the statistical uncertainty, while the shaded boxes correspond to the systematic uncertainty. The yellow band and colored curves serve as a comparison to different PDF sets [18, 19] and theory frame works [20, 21]. Note that the systematic uncertainties for the charged $W$ cross section ratios as a function of $\eta_e$ are well under control and we are dominated by our statistical precision. Further studies into the newly established $W$ boson reconstruction process [16, 17] should reduce the systematic uncertainties on the $W^{\pm}$ cross-section ratio dependence on the boson kinematics.

## 4. Summary

We have measured and presented charged $W$ cross section ratios from combined 2011 and 2012 proton-proton STAR data at $\sqrt{s} = 500/510$ GeV. The inclusion of this data into global PDF analysis should help constrain the sea quark distributions and provide additional insight into the $\bar{d}/\bar{u}$ ratio near the valance region. Furthermore, with the inclusion of the STAR 2013 data ($\sim 250$ pb$^{-1}$), we will be able to further improve on the precision of our charged $W$ cross section ratios.

## References

[1] J. Gao *et al.*, Phys. Rev. D, **89**, 3, 033009 (2014).

[2] S. Alekhin, *et al.*, arXiv:1410.4412 [hep-ph] (2015).

[3] R. D. Ball, *et al.*, The NNPDF Collaboration, arXiv:1410.8849 [hep-ph] (2015).

[4] J. Gao and P. Nadolsky, JHEP, **1407**, 035 (2014).

[5] R. S. Towell *et al.*, Phys. Rev. D, **64**, 052002 (2001).

[6] Wen-Chen Chang and Jen-Chieh Peng, *Progress in Particle and Nuclear Physics*, **79**, 95(2014).

[7] P. E. Reimer (SeaQuest), J. Phys. Conf. Ser. **295**, 012011 (2011).

[8] C. Bourrely and J. Soffer, Nucl. Phys. B **423**, 329 (1994).
J. Soffer, C. Bourrely, and F. Buccella, arXiv:1402.0514 (2014).

[9] K. H. Ackermann *et al.* (STAR), Nucl. Instrum. Meth. **A 499**, 624 (2003).

[10] L. Adamczyk *et al.* (STAR), Phys. Rev. D **85**, 092010 (2012).

[11] M. Anderson *et al.* (STAR), Nucl. Instrum. Meth. **A 499**, 659 (2003).

[12] M. Beddo *et al.* (STAR), Nucl. Instrum. Meth. **A 499**, 725 (2003).

[13] C. Allgower *et al.* (STAR), Nucl. Instrum. Meth. **A 499**, 740 (2003).

[14] T. Sjostrand, S. Mrenna, and P. Skands, *Pythia 6*, https://pythia6.hepforge.org.

[15] S. Agostinelli *et al.*, Nucl. Instrum. Meth. **A 506**, 250 (2003).

[16] S. Fazio and D. Smirnov (STAR), PoS, DIS2014, 237, (2014).

[17] S. Fazio (STAR), These Proceddings (2015).

[18] H. L. Lai *et al.*, Phys. Rev. D, **82**, 074024 (2010).



PoS(DIS2015)051

[19] C. Bourrely, F. Buccella, and J. Soffer, Eur. Phys. J. C 23, 487 (2002).

[20] J. Campbell, K. Ellis, and C. Williams, *MCFM - Monte Carlo for FeMtobarn Processes*, mcfm.fnal.gov.

[21] P .M. Nadolsky and C.-P. Yuan, Nucl. Phys. B **666**, 3 (2003).


PoS(DIS2015)051